Materials Letters 162 (2016) 250–253

Contents lists available at ScienceDirect

Materials Letters

journal homepage: www.elsevier.com/locate/matlet

Investigation of the bonding strength and bonding mechanisms of SOFCs interconnector–electrode interfaces

D.N. Boccaccini [a,*], O. Sevecek [b], H.L. Frandsen [a], I. Dlouhy [c], S. Molin [a], M. Cannio [d], J. Hjelm [a], P.V. Hendriksen [a]

[a] Department of Energy Conversion and Storage, Technical University of Denmark, Frederiksborgvej 399, DK-4000 Roskilde, Denmark
[b] Brno University of Technology, Institute of Solid Mechanics, Mechatronics and Biomechanics, Technická 2, 616 69Brno, Czech Republic
[c] Institute of Physics of Materials, Academy of Sciences of the Czech Republic, Zizkova 22, 616 62Brno, Czech Republic
[d] University of Modena and Reggio Emilia, Department of Engineering "Enzo Ferrari", Modena 42025, Italy

ARTICLE INFO

Article history:
Received 13 July 2015
Accepted 26 July 2015
Available online 31 July 2015

Keywords:
Schwickerath crack-initiation test
Three-point bending test
SOC interfaces
Metal–ceramic bond strength

ABSTRACT

The determination of the bonding strength (BS) between solid oxide cell (SOC) electrodes and metal interconnects (IC) is of importance since it can impact the SOC lifetime. There are several methods for determining the adhesion between ceramic and metal layers at the macro-scale level, but no standard technique for such measurement is available. In this work, the BSs between an anode support (AS) and three different cathodes with a SOC interconnect were tested in three point bending test configuration. An adaptation of the Schwickerath crack initiation test (SCIT) (ISO 9693) was used to verify its applicability for the determination of bonding strength in the interfaces. The results suggest that this test is a valid method for the mechanical characterization of SOC interfaces.

1. Introduction

The bonding between SOC electrodes and metal ICs is a critical issue, which may determine the stack lifetime [1]. An understanding of the bonding mechanism is essential to design successful IC-cathode/anode interfaces in SOCs. Metal–ceramic bonds, which occur during the ceramic firing, have been classified into three main categories: chemical bonding, mechanical interlocking and Van der Waals forces [2].

Although it is of importance to measure the interfacial crack resistance of a SOC [3,4], no standard technique for such measurements is available. Therefore, the objective of the present investigation is to explore the feasibility of utilizing the SCIT (ISO 9693), introduced in 1999 for dental ceramic–metal composites [5,6], for the determination of SOCs IC-cathode/anode BS. Despite the different material properties and geometries used in SOCs, the ceramic–metal bonding mechanisms are similar and then the evaluation of the bonding strength could be performed similarly. In this work the method is revised to deduce the contribution from the residual stresses (RS) on the strength separately, as the RS vary with temperature and time.

2. Experimental

Four different interfaces are investigated in this work: (A) IC-LSM cathode contact layer with LSCF:CGO cathode, (B) IC-LSC:CGO cathode; (C) IC-LSCF:CGO cathode and (D) inteconnect-3YSZ-Ni AS. Table 1 lists the main properties of the layers and materials on either side of the interface, while methods employed for their characterization and literature are reported elsewhere [7].

2.1. Materials

SOC cells were prepared and laser cut to the final dimension of (8 ± 0.1) mm × (3 ± 0.1) mm to measure the BS by the SCIT. The average thickness of the cells after the cathode deposition was (0.4 ± 0.01) mm. Commercially available ICs (Crofer 22 APU®) for SOFC with a thickness of (0.3 ± 0.01) mm were cut to dimensions (15 ± 0.1) mm × (3 ± 0.1) mm and assembled with the laser cut cells following the geometric configuration of the standard ISO 9693 as shown in Fig. 1.

2.2. Sintering

The specimens were fired at 930 °C for 24 h with heating and cooling rates of 2 °C/min. Loads (0.5 kg/cm^2) were applied outside the furnace and transmitted to the sample by an alumina rod to simulate the real compressive stresses in the stack. In the case of the anode-IC interface, the firing was performed under reducing

---

* Corresponding author. Fax: +45 4677 5858.
E-mail address: dinb@dtu.dk (D.N. Boccaccini).

http://dx.doi.org/10.1016/j.matlet.2015.07.137
0167-577X/© 2015 Published by Elsevier B.V.

Table 1
Summary of thermo-mechanical properties of SOFC layers for FEM simulation.

Layer name	Material	Thickness (μm)	Porosity	TEC(Averaged 25–900 °C) (10^{-6}/K)	E(GPa)	Layers contained in configurations
AS	3YSZ/NiO	290	0.11	13.1	157 ± 30	A, B, C
Anode	8YSZ/NiO	12.5 (10–15)	0.05	12.6	183 ± 20	A, B, C
Reduced AS	3YSZ/Ni	290	0.35	12.9	96 ± 42	D
Reduced anode	8YSZ/Ni	12.5 (10–15)	0.27[a]	12.5	100 ± 30*	D
Electrolyte	8YSZ	10 (9–12)	0	10.8	201 ± 14	A,B,C,D
CGO layer	CGO	5.5 (3–8)	0.20	12.5	106 ± 25	A,B,C
Cathode	LSCF:CGO	15–20	0.31	13.95	61 ± 27	A,C
Cathode	LSC:CGO	15–20	0.38	18.75	44 ± 17	B
Cathode contact layer	LSM	50	0.22	12.3	65 ± 19	A
IC Co layer	Co_3O_4	2.5	–	9	152 ± 19	A,B,C
IC Co reduced layer	Co	2	–	13	207 ± 20	D
IC spinel layer	$(Mn,Cr)_3O_4$	2	–	9	201 ± 13	A,B,C,D
IC metal	Fe Cr stainless steel	300	–	12.3	200 ± 14	A, B, C, D

[a] Estimated from the initial porosity.

conditions (9%H_2–N_2).The number of specimens prepared and tested was 15 for each type of interface investigated.

2.3. Three point bending test based on the ISO 9693 standard

A thermo-mechanical analyser (TMA) (TMA 402 F1 Hyperion) was used to perform the SCIT required for the determination of the BS. Fig. 1 shows the sample geometry and the test conditions scheme. The specimens were placed with the ceramic layer facing down in the bending apparatus. The sample was supported by rods 10 mm apart. The load is applied in the centre with aø2 mm rod displaced by a piston loading the sample with a rate of 0.025 N/min. In order to accomplish with the standard requirement, the value of the ratio $|\sigma_{xy}|/\sigma_{yy} \cong 1$ must be verified under pure mechanical loading. Then the bonding strength (τ) (MPa) is defined as the average value of $|\sigma_{xy}|$ for a load of 1 N in the region of positive stress σ_{yy} multiplied by F_{fail} [5,6].

$$\tau = \tau_{res} + \tau_{ext} \qquad (1)$$

where $\tau_{ext} = \sigma_{xy}(F_{fail})/(F_{FEM})$ and $F_{FEM} = 1$ N.

3. Results and discussion

Fig. 2 shows the variation of the load and deflection as function of time for representative samples during the 3PB test. Debonding occurs when there is a sudden drop in the displacement and afterwards the displacement rate follows that of the metal alone.

Finite Element (FE) analysis was used for the calculations of the RS. The FE model of the specimen (see Fig. 1) is initially loaded by change of the temperature from bonding temperature (930 °C) to the testing temperature (20 °C) (introducing RS) and subsequently subjected to the effects of the actual loading at failure and then insert in Eq. (1) to determine the BS. This analysis enables examination of the stress conditions near the edge of the bimaterial notch, where debonding of ceramic and metal usually starts.

The obtained BSs are reported in Fig. 3(a–c) together with the $|\sigma_{xy}|/\sigma_{yy}$ ratios. Fig. 3(a) shows that the RS in the anode are low due to good matching of TEC between AS and metal. In case of pure external mechanical loading, the anode can withstand higher load than the cathodes, because it is almost free of thermal stress. However, after the corrections of RS (combined loading), the actual bonding of the anode is lower than that of cathodes. The $|\sigma_{xy}|/\sigma_{yy}$ ratios for pure external mechanical loading are$\cong$1 for all the interfaces, which is a requirement of ISO 9693-1.

Fig. 4 shows fresh fracture surfaces on selected samples looking at the metal side. The white spots in the SEM pictures correspond to pieces of cathode material that remained bonded to the metal. A strong mechanical interlocking bonding was identified in the cathodes by nano-indentation testing and Scanning Probe Microscopy (SPM) imaging [7], e.g. LSM particles remained embedded into the scale layer during sintering, giving rise to mechanical interlocking.

Fig. 4 shows the high amount of bonded contact points between cathode and metal in LSC:CGO (the material showing the highest BS) and LSCF:CGO. Fig. 4 indicates a high uniformity of

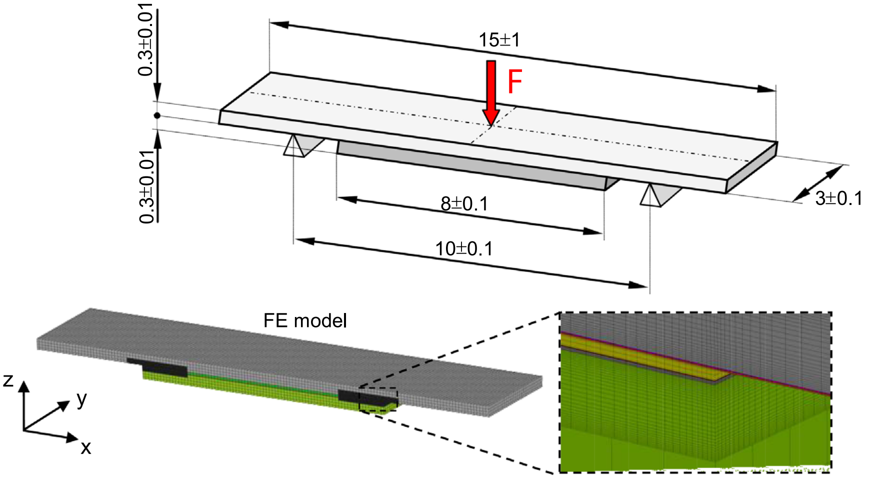

Fig. 1. Test specimen (FE model) configuration (adapted from ISO9693).